



Research on aluminum alloy hot stamping process using short-wave infrared heating technology

Qinghua Tang¹, Shengjie Yao^{1,2,†}, Xin Dong¹, Xiaofeng Wang¹, Deqi Hou¹, Long Zhao¹,
Shunhao Li¹ and Guannan Chu¹

¹*School of Materials Science and Engineering, Harbin Institute of Technology, Weihai, 264209, China*

²*Shandong Provincial Key Laboratory of Special Welding Technology, Harbin Institute of Technology, Weihai, 264209, China*

[†]*E-mail: shj_yao@163.com*

<https://homepage.hit.edu.cn/Yaoshengjie>

Nowadays, the increasing requirements for energy conservation and emission reduction have fostered the application of the hot-stamped aluminum alloy for lightweight. However, it is difficult to achieve industrialized production because of the long-term process as well as high production costs. In this study, a hot stamping process for aluminum alloys based on short-wave infrared heating is presented. To enhance the absorption of short-wave infrared rays, the emissivity was increased by nano-graphite coating, it greatly improved heating efficiency. U-shaped parts with different forming depths (20~60mm) were successfully prepared in 5052 aluminum alloy, and the larger strain in the sidewall region of the U-shaped parts resulted in higher strength and hardness. The increased deformation promotes dynamic recrystallization, the grain morphology shifts to equiaxed recrystallized grains, and a large number of low-angle grain boundaries are retained within the grains, indicating that dynamic recovery dominates the deformation mechanism.

Keywords: Aluminum alloys; Hot stamping; Short-wave infrared; Graphite coating; Deformation strengthening.

1. Introduction

In recent years, energy shortages and environmental pollution have become increasingly serious problems worldwide, and lightweighting of automobiles has distinct effect on energy-conservation and emission reduction effects [1]. The 5XXX series aluminum alloys belong to the non-heat-treatable reinforced aluminum alloys, they are widely used in the automotive and shipbuilding industries due to their advantages of being lightweight, having high strength, and good corrosion resistance. Figure 1 illustrates the lightweighting potential of various metal materials arranged according to their specific strength [2]. However, the forming performance of aluminum alloy is poor at room temperature, and cold stamping is prone to defects such as rupture, wrinkling, and springback, making it difficult to form complex parts. Hot forming can effectively improve the forming performance of aluminum alloys and control springback to enhance forming accuracy. The

[†]Work partially supported by National Natural Science Foundation of China (Grant No.52275319); Natural Science Foundation of Shandong Province (ZR2020ME146); Key Research and Development Project in Shandong Province (2021SFGC0902).

© The Author(s) 2024

Y. Zhang and M. Ma (eds.), *Proceedings of the 7th International Conference on Advanced High Strength Steel and Press Hardening (ICHSSU 2024)*, Atlantis Highlights in Materials Science and Technology 3,

https://doi.org/10.2991/978-94-6463-581-2_28

traditional aluminum alloy hot stamping process has long solid solution and aging cycles [3], resulting in low productivity and high production costs.

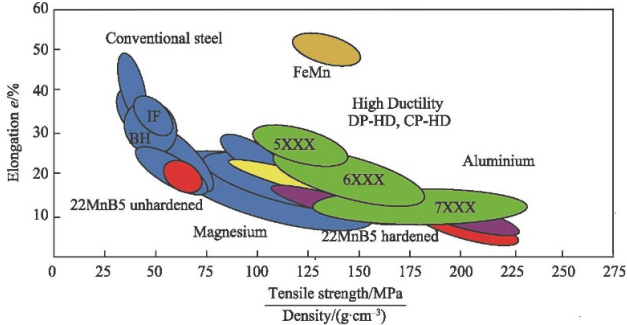


Fig. 1. Lightweight design potential of metallic materials.

The mainstream heating methods for aluminum alloy sheet forming are convection heating and radiation heating [4], they are not only inefficient but also have high energy-consumption. The short-flow process for aluminum alloys lies in the use of new heating methods. Short-wave infrared radiation is a type of electromagnetic radiation. The principle of infrared heating is based on resonating the free electron collective on the surface of the metal by incident light [5]. Short-wave infrared heating has considerable potential in aluminum alloy hot stamping processes, especially with surface coating technology that modulates the surface absorptivity rate. The aim of this work is to improve heating efficiency by increasing the emissivity/absorptivity of the aluminum alloy surface and to achieve customized temperature fields. The effects of various infrared heating processes on the mechanical properties of stamped parts are investigated in detail.

2. Material and Methods

The aluminum alloy used for the hot stamping experiments in this research is commercial 5052 aluminum alloy (H32) with thickness of 2 mm, and the chemical composition is shown in Table 1.

Table 1. Chemical composition of 5052 aluminum alloy(wt%).

Element	Si	Fe	Cu	Mn	Mg	Cr	Zn	Ti	Al
Content	0.1734	0.2311	0.0098	0.0321	2.5058	0.2002	0.0219	0.0292	Bal.

The surface absorptivity of the bare sheet and the coated sheet were measured using a Shimadzu UV3700 spectrophotometer. As shown in Fig. 2, the surface absorptivity of bare sheet was about 10% in the short-wave infrared wavelength range (1.4 μm-1.7 μm), while the surface absorptivity of the coated sheet was about 75%.

The infrared-heated blanks are quickly transferred from the heating platform to the mould for press hardening, and the U-shaped die is rapidly closed to minimize temperature dissipation. The heating process is monitored by a paperless recorder connected to a type K thermocouple to track temperature changes. Figure 3 shows that graphite coating can substantially improve heating efficiency.

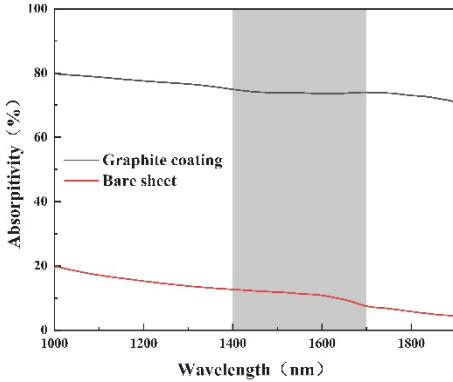


Fig. 2. Absorptivity of bare sheet and graphite coating.

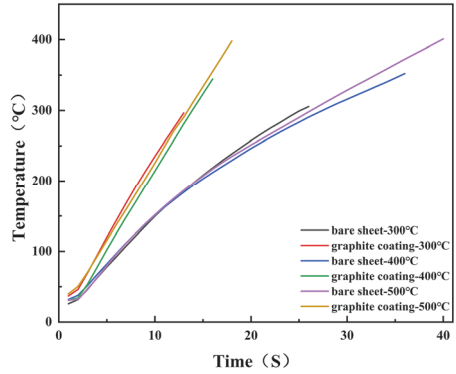


Fig. 3. Comparison of temperature rise rates for bare sheet and coated sheet.

Using infrared heating, the blanks were heated to 300°C, 350°C, and 400°C. U-shaped parts with forming depth varying from 20 mm to 60 mm were then stamped, as shown in Fig. 4.

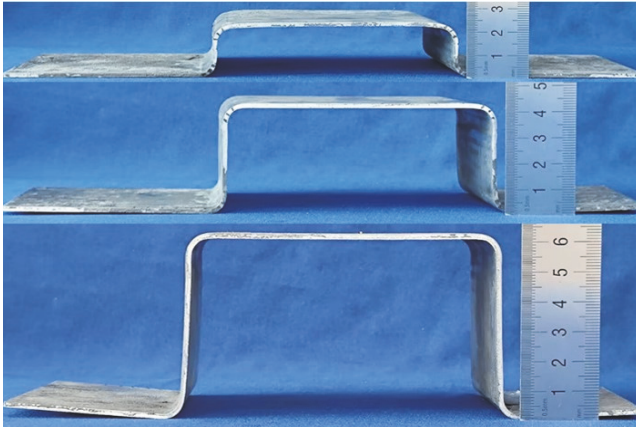


Fig. 4. U-shaped parts with different forming depths.

Uniaxial tensile tests were carried out on an MTS-100kN universal testing machine at a strain rate of 0.6 mm/min, and the strain was calculated using the Digital Image Correlation (DIC) method. The samples were mechanically ground and polished, electrolytically corroded with 10 vol% HClO₄ + 90 vol% C₂H₅OH mixture solution, and EBSD observation of microstructure was carried out on the scanning electron microscope Zeiss SIGMA 500.

3. Results and Discussion

3.1. Mechanical properties

Vernier calipers were used to measure the wall thickness distribution along the side of the U-shaped part. The results, shown in Fig. 5, indicate that the sidewall region of the U-

shaped part experiences the largest amount of thinning and also has the highest Vickers hardness value, as depicted in Fig. 6. The 5XXX series aluminum alloys belong to the non-ageable strengthened aluminum alloys, and deformation strengthening is the primary method. Therefore, the degree of deformation largely determines its mechanical properties.

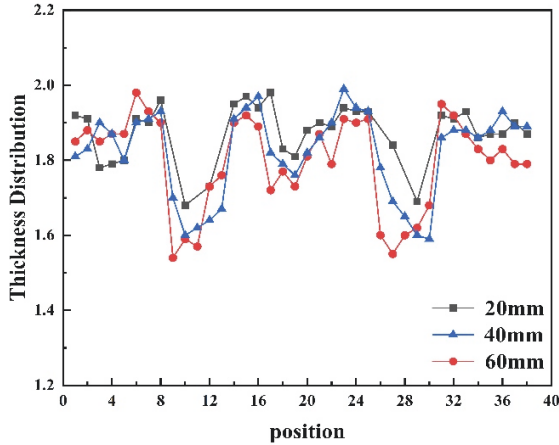


Fig. 5. Wall thickness distribution of U-shaped parts with different forming depths.

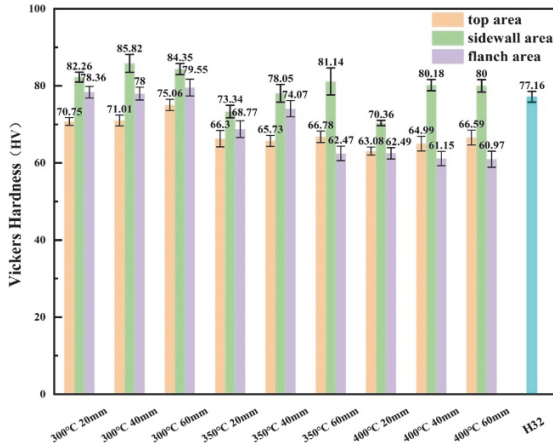


Fig. 6. Micro-Vickers hardness of different regions of U-shaped parts.

Figure 7 presents the stress-strain curves from uniaxial tensile tests. For the U-shaped parts with different forming parameters, only the sidewall area, which undergoes significant thinning, has a higher tensile strength than the original state (229.51 MPa), indicating the characteristics of a hardened state. The other locations exhibit the characteristics of a softened state, with a slight reduction in strength and an increase in elongation compared to the original state (14.51%).

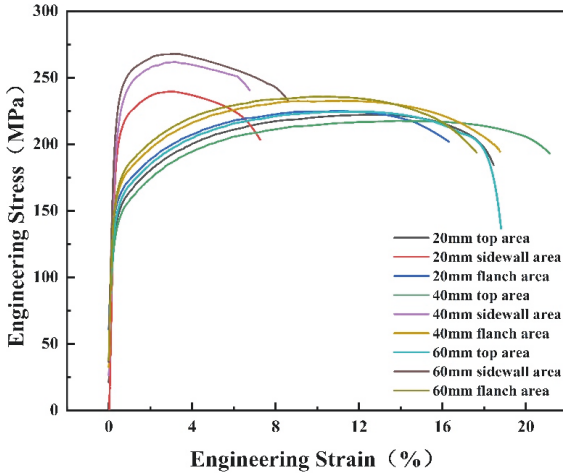


Fig. 7. Stress-strain curves in different regions of U-shaped parts.

3.2. Microstructural evolution

Figure 8 shows the grain orientation distribution (IPF) and the grain size distribution curves in the sidewall region of U-shaped parts with different forming depths. Figure 8(a) presents the microstructure of 5052 aluminum alloy in the original state (H32), where the grains are significantly elongated along the rolling direction, showing a slender fibrous shape. As the forming depth increases, the thinning in the sidewall region becomes more pronounced, and the grain morphology changes from strip-rolled grains to equiaxed recrystallized grains. Plastic deformation promotes recrystallization. However, aluminum alloys are high stacking fault energy metals, making their recrystallization relatively difficult to achieve. Therefore, the degree of grain refinement under small deformation is minimal. When the forming depth reaches 60 mm, the number of recrystallized grains further increases, resulting in a certain degree of grain refinement, and the average grain size decreases to 8.9 μm . In addition, the plastic deformation during the stamping process induces intragranular slip, leading to the rotation of the grains, and thus a change in orientation occurs.

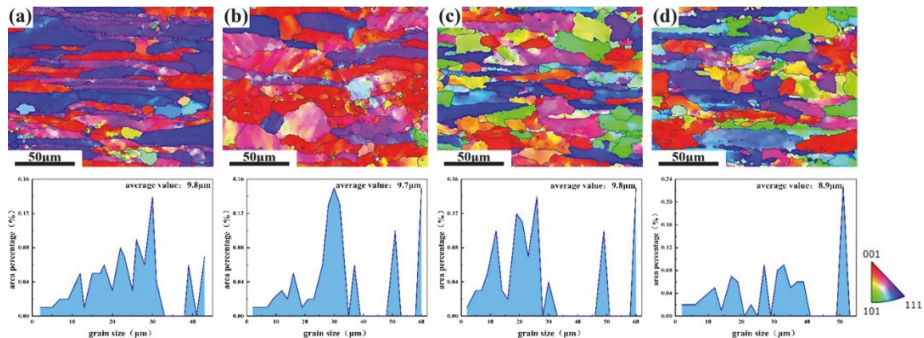


Fig. 8. Grain orientation distribution and grain size distribution curves of U-shaped parts with different forming depths. (a) original microstructure (b) 20mm forming depth (c) 40mm forming depth (d) 60mm forming depth.

Figure 9 shows the distribution of grain boundaries in the sidewall area with different thinning amounts and the distribution of grain orientation differences. There are a large number of low-angle grain boundaries within the grains. During the press forming process, the dislocation density increases and becomes entangled, forming a dislocation wall. This wall can form sub-grain boundaries, and can be retained within the grains. This indicates that dynamic recovery predominates in the deformation mechanism.

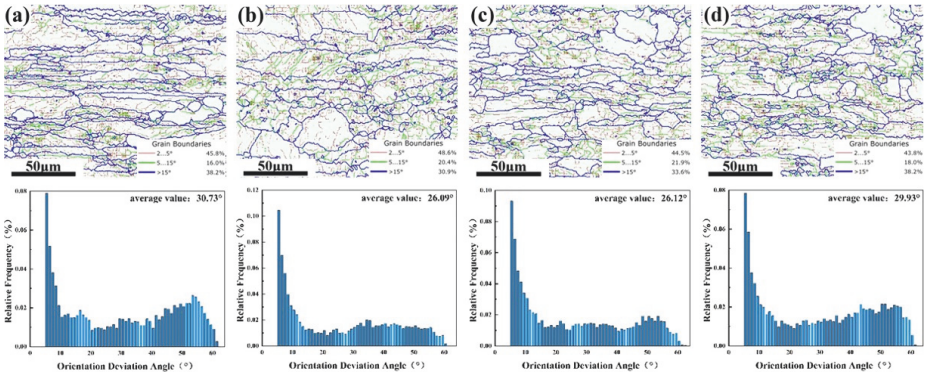


Fig. 9. Distribution of grain boundaries and grain orientation difference in U-shaped parts with varying thinning amounts. (a) original microstructure (b) 7.375% (c) 12.95% (d) 21.3%.

Short-wave infrared heating can rapidly warm the aluminum alloy sheet to 300°C within 15 seconds. The blank experiencing short-time heating, will undergo a certain degree of recovery recrystallization. When the forming depth of the U-shaped part is 20 mm, the thinning of its sidewall area is 7.375%. At this time, the percentage of high-angle grain boundaries decreases to 30.9%, the percentage of low-angle grain boundaries rises to 69.1%, and the average orientation deviation angle decreases to 26.09°. The plastic deformation during the stamping and forming process leads to a gradual increase in the sub-crystalline structure within the grains. This process as a whole is a combination of dislocation recombination disappearance and formation regeneration. For a thinning of 7.375%, the proportion of newly formed sub-crystals is higher than the proportion of sub-crystals converted to recrystallization.

When the forming depth of the U-shaped part reaches 40 mm, the thinning of its sidewall area is 12.95%. At this time, the percentage of high-angle grain boundaries increases to 33.6%, the percentage of low-angle grain boundaries decreases to 66.4%, and the average orientation deviation slightly increases to 26.12°. Dynamic recrystallization during the forming process was further promoted due to the increased deformation. The relative transformation from low-angle grain boundaries to high-angle grain boundaries increased. The amount of thinning ranged from 7.375% to 12.95%, there exists a balanced state between the proportion of newly formed sub-crystals and that of sub-crystals converted to recrystallization.

When the forming depth of the U-shaped part reaches 60 mm, the thinning in the sidewall area is 21.3%. With further deformation, the proportion of high-angle grain

boundaries increases, the proportion of low-angle grain boundaries decreases, and the orientation deviation angle becomes larger.

4. Conclusion

In this work, aluminum alloy blanks were heated using short-wave infrared radiation technology and then hot stamped to form U-shaped parts with different depths. The main conclusions are as follows:

(1) Graphite coating can substantially increase the absorption rate of infrared rays on the surface of aluminum alloy, and the heating efficiency of aluminum alloy sheet can be increased by more than 50% with the assistance of graphite coating.

(2) The U-shaped parts formed by hot stamping showed the highest thinning in the sidewall region, corresponding to the highest micro-Vickers hardness value. The other regions exhibited softening characteristics, with reduced strength but increased elongation.

(3) With increasing deformation, the grain morphology changes from strip-rolled grains to equiaxed recrystallized grains. A large number of low-angle grain boundaries are retained within the grains, and dynamic recovery dominates the deformation mechanism.

References

1. W. L. Sun, X. K. Chen, L. Wang, Analysis of energy saving and emission reduction of vehicles using light-weight materials, *Energy Procedia*. 88:889—893(2016).
2. J. Schlosser, R. Schneider, W. Rimkus, Materials and simulation of a crash-beam performance: A comparison study showing the potential for weight saving using warm-formed ultrahigh strength aluminum alloys, *Journal of Physics: Conference Series*. 896(1):012091(2017).
3. X. Xu, Y. Zhao, X. Wang, The rapid age strengthening induced by Ag additions in 7075 aluminum alloy, *Materials Science and Engineering: A*. 648:367—370(2015).
4. K. Lin, B. B. You, G. W. Xie, High-strength aluminum alloy hot stamping process & numerical simulation, *Automobile Technology & Material*. (9):1—5(2020).
5. M. Biesuz, T. Saunders, D. Ke, M. J. Reece, C. Hu, S. Grasso, A review of electromagnetic processing of materials (EPM): heating, sintering, joining and forming, *Journal of Materials Science and Technology*. 69:239—72(2021).

Open Access This chapter is licensed under the terms of the Creative Commons Attribution-NonCommercial 4.0 International License (<http://creativecommons.org/licenses/by-nc/4.0/>), which permits any noncommercial use, sharing, adaptation, distribution and reproduction in any medium or format, as long as you give appropriate credit to the original author(s) and the source, provide a link to the Creative Commons license and indicate if changes were made.

The images or other third party material in this chapter are included in the chapter's Creative Commons license, unless indicated otherwise in a credit line to the material. If material is not included in the chapter's Creative Commons license and your intended use is not permitted by statutory regulation or exceeds the permitted use, you will need to obtain permission directly from the copyright holder.

